Journal of Mechanical Engineering *Vol 14(1), 97-112, 2017*

Numerical Simulation of The Femur Fracture With and Without Prosthesis Under Static Loading Using Extended Finite Element Method (X-FEM)

*Zagane Mohammed El Sallah**
Benbarek smail
Benouis Ali
Sahli Abderahmen
Bachir Bouiadjra bel abbes
Boualem Serier
LMPM, Department of Mechanics, Faculty of Engineering
University of Sidi Bel Abbes, BP 89
City Ben M'hidi, Sidi Bel Abbes 22000, Algérie

ABSTRACT

The strength of the bone depends on its mineralization state and its geometry, which depend on the loads supported. Thus the bone optimizes its mass and its geometry through the process of remodeling and improves its lift. This phenomenon can be altered by metabolic imbalances such as fall or trauma. The result is fractures, the most important of which are the proximal femur. The direct consequence of this type of fracture is the replacement of the joint by a Total Hip Prosthesis (PTH). The number of prosthetic implantations continues to increase given the longer life expectancy of patients.. This study is to compare the modeling to identify regions of fracture risk of femur and after the location of the total hip prosthesis (THP) by the extended finite element method (X-FEM) under static stress for a deferent orientation loading and for two materials (isotropic / orthotropic). The results show that the distribution of von mises stresses in the components of the femoral arthroplasty depends on the material and the design of the stem and show that the vertical loading leads to fracture of the femoral neck and the horizontal loading leads to the fracture of diaphysis femoral. The isotropic consideration of bone leads to bone fracture by propagation of the fissure, but the orthotropic consideration leads to the fragmentation of the bone. This modeling will help

ISSN 1823- 5514, eISSN 2550-164X
Received for review: 2016-08-02
Accepted for publication: 2017-04-13
Published: 2017-06-15

to improve the design of the indoor environment to be safer for the means of passenger transport.

Keywords: *Femur, Fracture, Total Hip Prosthesis (THP), Static, Extended Finite Element Method (X-FEM).*

Introduction

The femur is the longest, strongest and heaviest bone in the human body [1,2,3]. Each year, more than 1.17 million people die in circulation accidents in the world. 65% of deaths are pedestrians. In 2005 mortality after 1 year hip fracture is approximately 22% for men and 14% for women [4]. On the other had 90% of fractures are the result of falling with provoke mostly the fracture of the intertrochantérienne region of the femur [5].

Total Hip Prosthesis (THP) has been an extremely effective procedure for relieving pain and dysfunction in patients with hip arthritis of various aetiologies. However, after many decades of total hip replacement, there has also been a substantial increase in the incidence of peri-prosthetic fractures after THP, with over 800,000 hip replacements performed annually [6,7]. Among these fractures, fractures of the femoral neck (hip joint) are the most recurrent and involve the replacement of the total hip joint by a mechanical joint THP.

The increase in the prevalence of fracture is attributed to the substantial increase in the number of primary and revision THAs performed annually, to the increasing number of patients with THP in place for more than 20 years, to the aging population of THP, poor bone quality and a high risk of fall), and broader indications for THP that enable younger, more active and therefore high-energy trauma sufferers to undergo surgery.

The objective of this work is to develop a numerical model to predict the fracture of the femur with and without a total hip replacement (THR), compare the behavior of the femur fracture with different materials properties (isotropic/orthotropic) and loads (resembling different falls), with the extended finite element method (XFEM).

XFEM is used to predicted the femur fracture and determine the location of crack initiation and the path of crack propagation include in Abaqus software.

Many of the works studied presented the femur, fracture of the patient after the Total hip replacement depend on the timing of the fracture, the type of fracture, and the stability of the implant [8,9,10].

The total hip joint's numerical model: bone (the human femur is given by Pacific Research Labs [11]). The three dimension reconstitution of all parts are realized separately and assembled.

The obtaining of the 3D solid model of the patient's femur is done by taking images of the interesting regions using the medical imaging technique (CT-scan). The thickness of each slice is about 1 mm for the proximal part until the small trochanter and 8mm from the small trochanter to the most distal of the shaft. Using the brightness of the tomographic shots, two regions can be distinguished: Cortical bone and cancellous bone. The three dimension reconstitution of both parts is realized separately (Figure 1) shows the steps of the 3D reconstitution of the femur.

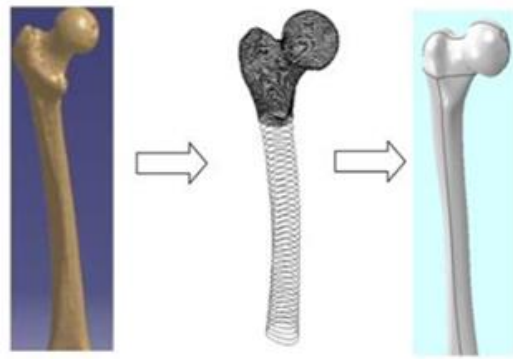

Figure 1: Femur 3D reconstitution procedure.

The Charnley-Muller-Kerboul third generation (CMK3) prosthesis is designed using the Solidworks Software and includes the assembly of all parts of the prosthesis into one CAD model in Figure 2.

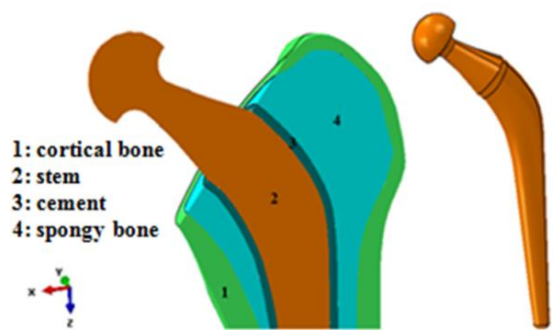

Figure 2: Three dimensional for longitudinal section of the reconstruction prosthesis.

Materials and methods

Materials

Bone composed of two components (cortical and spongious) which differ in their behavior. The mechanical properties of the materials are taken from previous studies [12,13,14]. For the first step, the cortical and spongious bone has been defined as isotropic linear materials are given in Table 1 and linear orthotropic for the second step in Table 2.

Table 1: Material properties used in the simulation

Materials	**Young's modulus E (GPa)**	**Poisson ratio υ**	**Yield Strength (GPa)**	**Ultimate Tensile Strength (GPa)**	**Reference**
stem stainless steel 316 L	210	0.3	0.455	0.65	Br.(2000)and Kayabasi, 2006 [15]
Cortical bone	17	0.36	0.17	0.035	Monif, M.M. (2012) [16]
Bone Cement	2	0.38	0,0438	0.0353	Darwish, S.M (2009) [17], and Bergmann, G. (2001) [18]
Cancellous Bone	0.6	0.3	0.00389	-	Darwish, S.M (2009) [17], and Bergmann, G. (2001) [18]

Table 2: Elastic properties of orthotropic bone

E_1 (Gpa)	**E_2 (GPa)**	**E_3 (GPa)**	**G_{12} (GPa)**	**G_{23} (GPa)**	**G_{31} (GPa)**	**υ_{13}**	**υ_{23}**	**υ_{12}**
16.6	17.0	25.1	7.2	8.4	7.1	0.23	0.24	0.33

Directions 1, 2, 3: show radial circumferential and longitudinal directions respectively. E: the modulus of elasticity; G: the shear modulus; υ: Poisson's ratio.

Methods

FE model of the human femur was subjected to three loads in three different directions (Figure 3(a)).The applied load is 18 KN on the head of femur and the fixation of the femoral epiphysis was considered [19]. The model in this study is discretized by using tetrahedral elements. The complete Charnley model CMK3 (PTH, bone cement and femur) has in total 92530 elements shown in Figure.3.B.

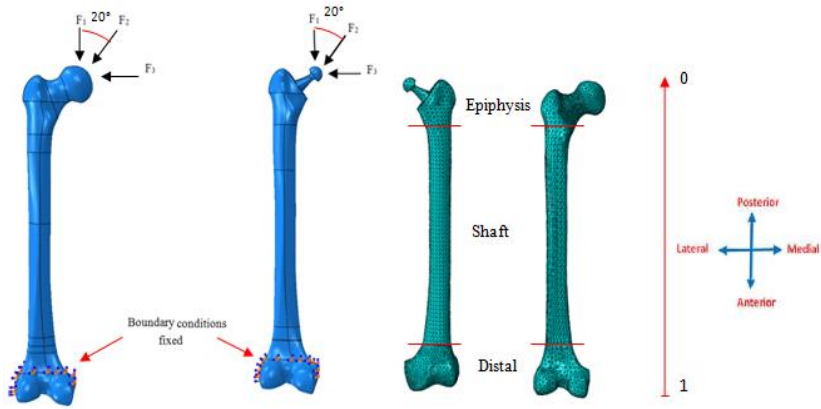

(a) (b)

Figure 3: (a) Representation of boundary conditions and loads applied to the applied force of the femur bone and femoral prosthesis. (b) finite element meshes on the femoral prosthesis and femur.

The extended finite element method (X-FEM) firstly introduced by Belytschko and Blackard, 1999 [10] to analyse the crack growth using finite elements with minimum remeshing. Numerous studies had examined the factors influencing the femur fracture his techniques. Some of them implemented the X-FEM technique to study the bone fracture [14,20,21,22].

Bone fracture analysis using the extended finite Element Method (XFEM) in Abaqus can be used to predict fracture behaviour of bone tissue to suggest surgical treatment options and take preventative measures. XFEM is a technique to model the location of crack initiation and the path of crack propagation without a priori knowledge of crack path

XFEM applies energy-based fracture criteria to determine the crack growth through a structure, and is not required to trav-el along specific element boundaries. This novel approach was used to predict fracture patterns in subjects with varying geometry and bone quality. Crack initiation occurred in elements when principal strains exceeded 0.61% [23]. The maximum principal stress criterion can be represented as:

$$\left\{ \frac{\sigma_{max}}{\sigma^{0}_{max}} \right\} \quad (1)$$

Here, σ0max represents the maximum allowable principal stress. The symbol<> represents the Macaulay bracket with the usual interpretation (i.e.,$<\sigma_{max}>= 0$if $\sigma_{max}< 0$ and $< \sigma_{max} > = \sigma_{max}$ if $\sigma_{max} \geq 0$). The Macaulay brackets are used to signify that a purely compressive stress state does not initiate damage. Damage is assumed to initiate when the maximum principal stress ratio (as defined in the expression above) reaches a value of one [24]. The parameters required by the X-FEM for models were selected on the basis of experimental data from the literature Table 3 [25].

Table 3: X-FEM damage parameters

Bone properties		
σ_{nc} (Mpa)	**G_{nc} (N/mm)**	**G_{sc} (N/mm)**
116	1.16	2.97

σnc: the normal strength; Gnc: fracture toughness for opening mode; Gsc: shear mode.

Results and Discussion

The results presented in Figures 5 and 6 show the results of the femur fracture under three different loading directions (F1, F2, F3), for healthy and with the implant model and for both isotropic and orthotropic mechanical property of the considered bone.

In the first load case (F1); one can see the crack initiation in the femoral neck region in a plane parallel to the femoral neck section leading to a complete fracture of the femoral neck.

In the case of the second loading; it was found that the initiation of the fracture takes always the region of the femoral neck as an initiation area. This type of force slightly affects the behaviour of the fracture. One notices a slight difference of the fracture relative to the first case, which approximates the femoral head. For the case of a thigh bone with implant, it will usually cause the fracture to propagate through the femoral diaphysis.

Load F3: In this latter case, fractures propagate through the femoral shaft in its lower part flow third horizontal path in the shaft section for the two models (healthy femur and with the implant) and resulting from the complete fracture of the shaft femur.

For the case of orthotropic material, the crack initiates in the femoral neck, but this time we see two cracks. The main one propagates in the section of the neck and the second crack propagate in the same neck with an offset

from the first one and for the femur with implant case, the crack gives a fragmented bone fracture in the middle of the femoral diaphysis as shown in Figure 6.

For the second case, it was observed that the initiation and propagation of a single fracture close to the femoral head. In the implanted femoral case the crack initiates in the third distal part of femoral diaphysis and always gives fragmentation.

In the last case (for orthotropic material); a complex fragmentation is observed for both cases: femur and femur with implant. In this case it is considered that, in reality, there is a complete bone fragmentation in this area. Figures 7 and 8 show the variation of the Von Mises constraints for different perspectives: (lateral, anterior, posterior and medial) for the femur before and after THP.

In the non-prosthetic femur, the force applied to the femoral head is transmitted to the level of the femoral neck to reach the diaphysis. Thus, the distribution of the Von Mises stresses at the diaphysis on the medial side varies between 1350 MPa to 250 MPa for the load F1 and F3. At the neck, the maximum stress of Von Mises ranges from 50 MPa to 800 MPa for the load F2. The stress is less important than in the posterior face varies between 50 MPa and 350 MPa for the epiphysis part.

For the prosthetic femur, the distribution of the von Mises stress is observed at the diaphysis on the medial side, ranging from 325 MPa under the neck of the prosthesis to 400 MPa at the tip of the implant. Conversely, on the lateral face, the Von Mises stresses vary from 160 MPa at the trochanters to 110 MPa at the tip of the implant for the loads F1 and F3. On the other hand the charge F2, produces high stresses in the area of the epiphysis on the medial side, varies between 270 MPa and 50 Mpa.In the isotropic case we note that the stress constraint strongest of orthotropic materials.

The bone strong in one direction and very weak for the two remaining directions. This difference leads to a couple of bone around the main direction under the different loading. This combined torque bending tension is the parameter responsible for the fragmentation of the femur.

Comparison between predicted and experimental complete fracture pattern is given in Figure 4. One can notice that a very good agreement is obtained between the predicted and experimental patterns, directed by Azhar.A.Ali, 2014 [26] and Jai Hyung Park. et al., 2016 [27].

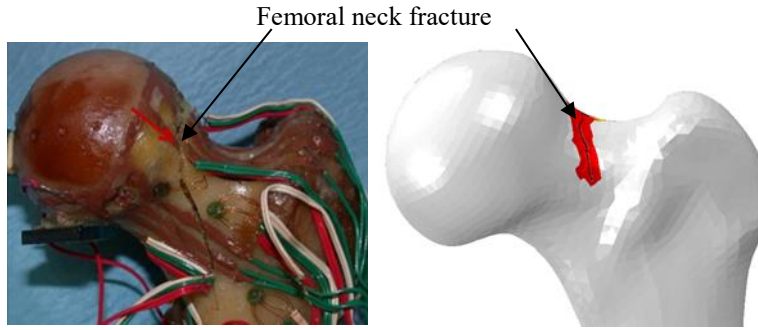

Figure 4: Comparison between the location of the fracture with simulation results (a) and experimental (b) [26].

With implant	Without implant
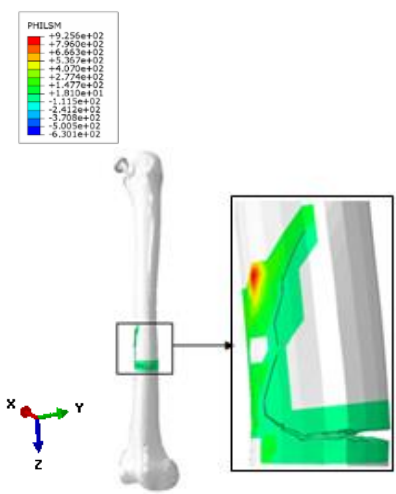	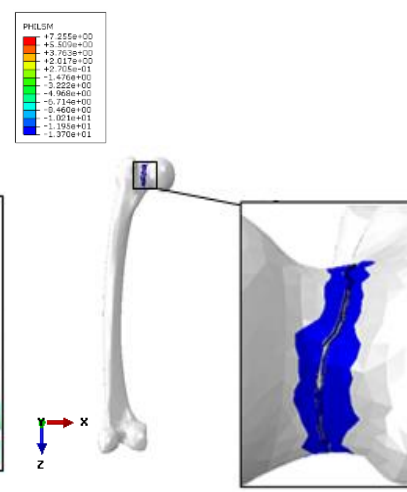
Load F1	

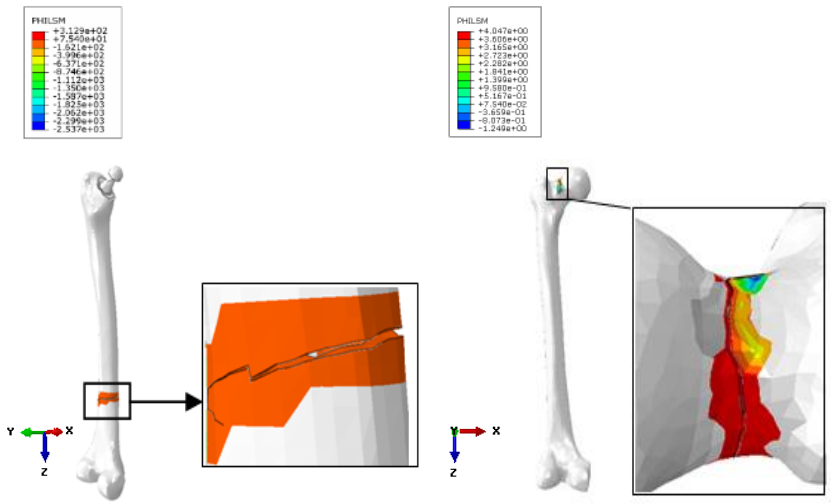

Load F2

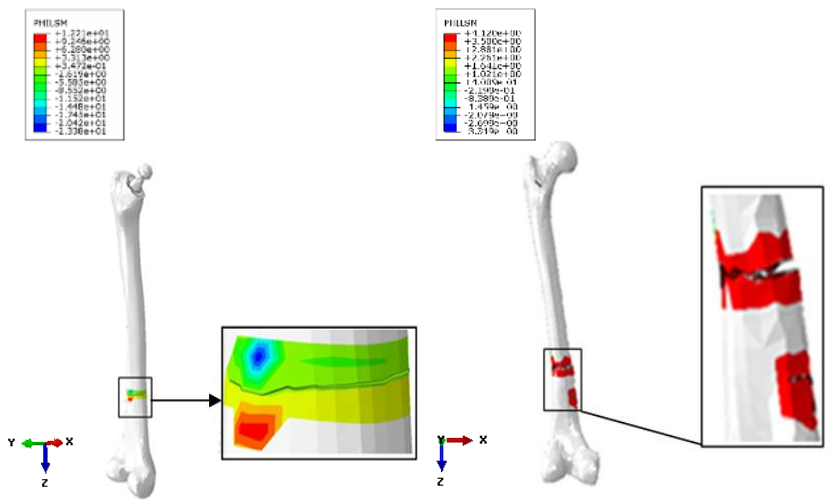

Load F3

Figure 5: Comparison of the fracture between femur and PTH for three load cases in materials isotropic.

With implant	Without implant
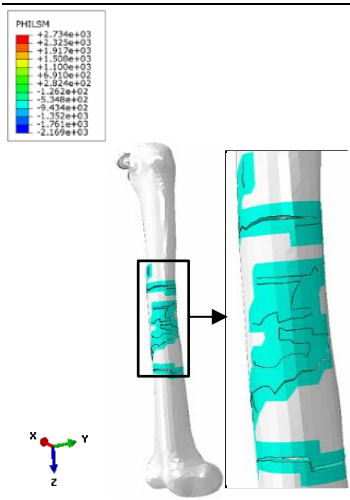	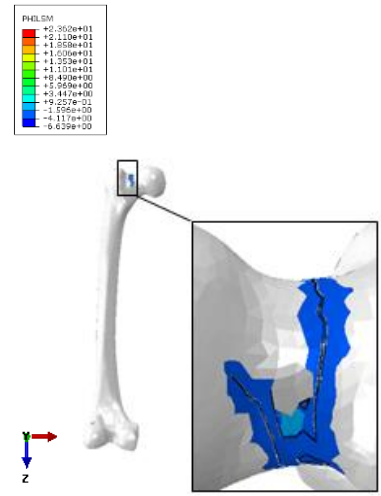
Load F1	
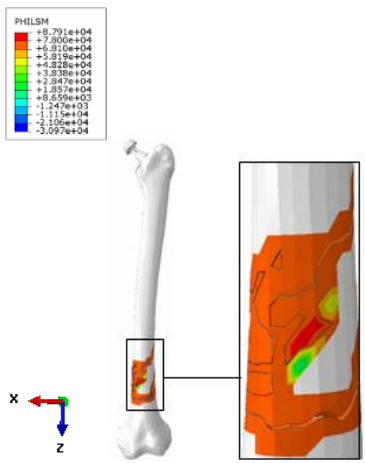	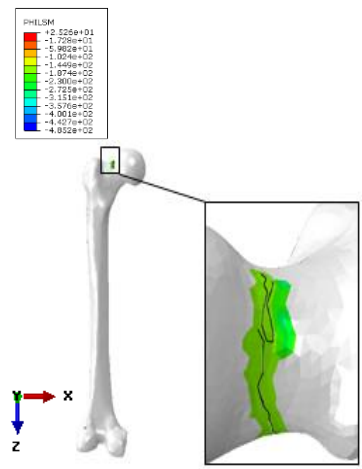
Load F2	

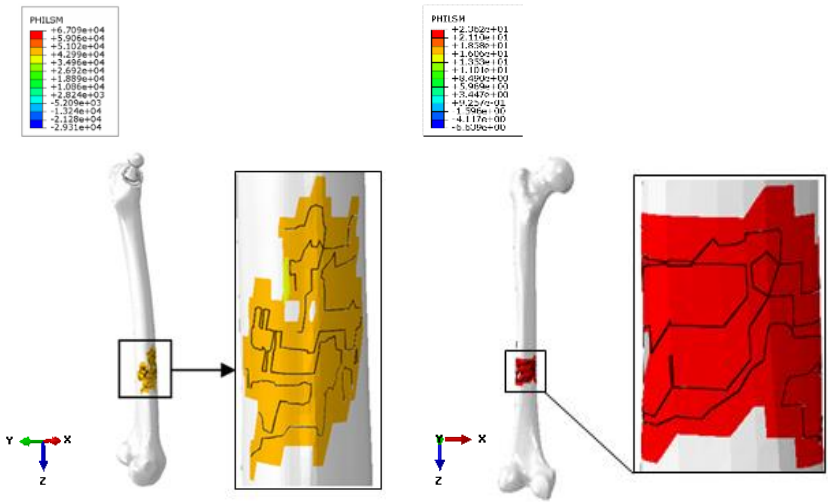

Load F3

Figure 6: Comparison of the fracture between femur and PTH for three load cases in materials orthotropic.

Isotropic materials	Orthotropic materials

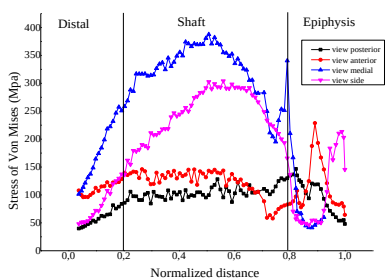

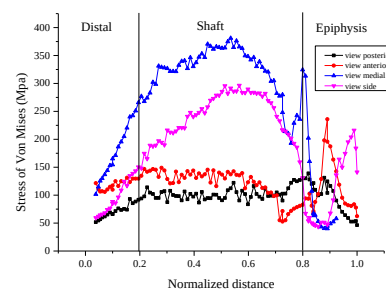

Load F1

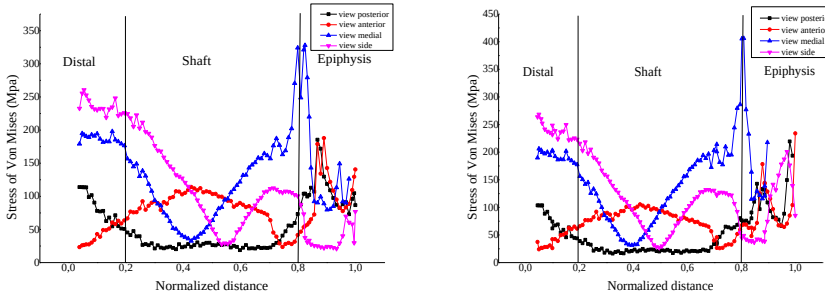

Load F2

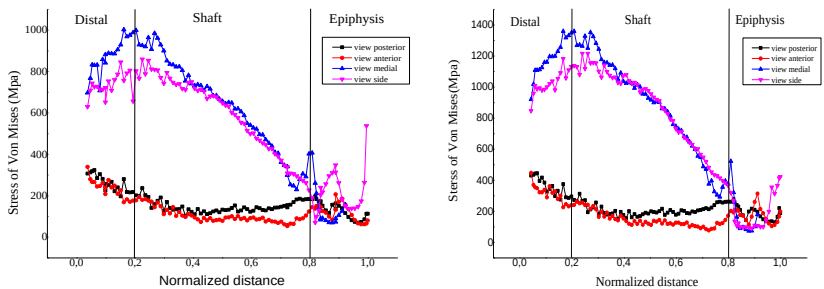

Load F3

Figure 7: Von mises stress distribution of the bone femur between the two materials for three load cases.

Isotropic materials	Orthotropic materials
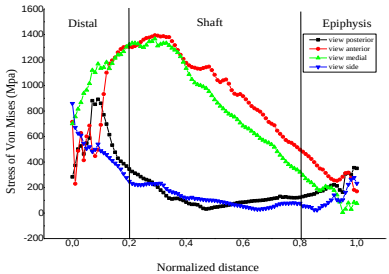	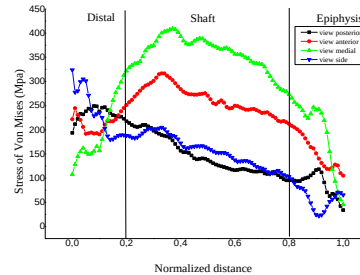
Load F1	
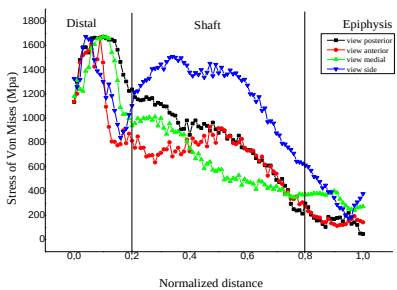	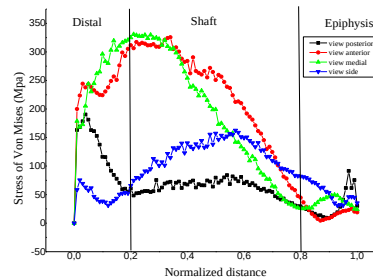
Load F2	
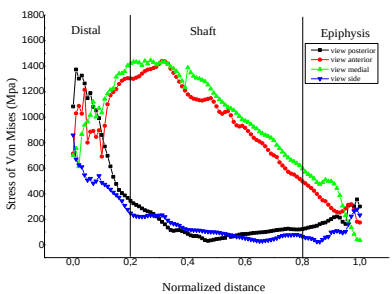	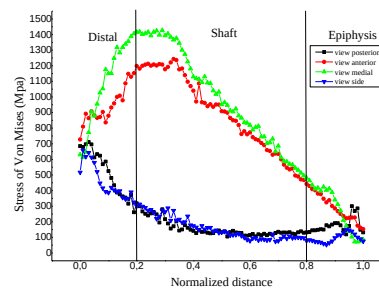
Load F3	

Figure 8: Von mises stress distribution of the bone femur with implant between the two materials for three load cases.

Conclusions

The development of a FE model to predict human femoral fractures is a novel treatment and preventative care approach for clinic care population. The fracture prediction model should provide clinicians and therapists within an accurate representation of what kind loading conditions that have potential to causes human bone fracture as well as the fracture location and type. X-FEM allows the prediction of the initiation and propagation of cracks without prior knowledge of the path of the crack.

Modeling results of the femur fractured show that the considered material's properties (isotropic / orthotropic) of cortical bone affected the nature of the fracture type (fragmentation our fracture). The location of the fracture has a relationship or depends on the nature of shock.

The direction of loading (20 ° – vertical – horizontal) determines the fracture zone of the femur (neck fracture our diaphysis). The modeling can predict the exact cause of the fracture trauma, which can be useful in clinical findings.

References

[1] Whittle, AP. 2003. Wood II GW: Fractures of lower extreme ty. In: Canale TS (ed.): Campbell's Operative Orthopaedics. 10th ed. Vol. 3. pp.2825-2872, Mosby, St Louis London Philadelphia Sydney Toronto.

[2] Platzer, W. 2003. Color Atlas of Human Anatomy. Vol. I. Locomotor System. 5th ed. Thieme Verlag, Stuttgart New York.

[3] Bucholz, R.; Brumback, R.1996. Fractures of the shaft of the femur. In: Rockwood C, Green D, Bucholz R et al. (eds.): Rockwood and Green's Fractures in Adults, 4th ed. Pp. 1827-1918, Lippincott-Raven, Philadelphia.

[4] Brauer, C.; CocaPerrailon, M.; Cutler, D.M., Rosen, A.B. 2009. Incidence and mortality of hip fractures in the United States. J. Am. Med. Assoc. 302,1573–1579.

[5] Cummings, S.R.; Melton, L.J. 2002. Epidemiology and outcomes of osteoporotic fractures. Lancet 359, 1761–1767.Yoon, Y.; Cowin, S. 2008. An estimate of anisotropic poroelastic constants of an osteon. Biomech Model Mechanobiol 7(1):13–26.

[6] M, Jasty.; W.J, Maloney.; C.R, Bragdon.; D.O, O'Connor.; T, Haire and H.H. 1991. The initiation of failure in cemented femoral components of hip arthroplasties, J Bone Joint Surg Br 73B, 551–558.

[7] W.J. Maloney.; J, Murali.; D,W. Burke.; D.O, O'Connor.; C, Zalenski and E.B, Braydon. 1989. Biome-chanical and histo-logic investigation of cemented total hip arthroplasties,Clin Orthop Rel Res 249 , 129–140.

[8] Ran Schwarzkopf, M.D.; M.Sc.; Julius K. Oni, M.D.; and Scott E.

Marwin, M.D. 2013 .Total Hip Arthroplasty Peripros-thetic Femoral Fractures A Review of Classification and Current Treatment. Journal of Bulletin of the Hospital for Joint Diseases, 71(1):68-78.

[9] James M, Gregory.: MD, Jason Hsu.; MD, and Leesa, M.; Galatz, MD. 2014. Periprosthetic humeral fractures in shoulder arthroplasty. journal of seminars in arthroplasty. 25, 59 – 6 3.

[10] Belytschko, T.; Black, T. 1999. Elastic crack growth in finite elements with minimal remeshing. Int J N mer Meth Eng 45(5):601–620.

[11] Pacific Research Labs. Biomed Town.https://wwwbiomedtown.org/

[12] Abderahmen Sahli, Smail Benbarek, Steven Wayne, Bel-Abbes Bachir Bouiadjra and Boualem Serier. 2014. 3D crack behavior in the orthopedic cement mantle of a total hip replacement. Applied Bionics and Biomechanics 11 135–147.

[13] S, Benbarek.; B, Bouiadjra.; T, Achour.; M, Belhouari.; B, Serier. 2007. Finite element analysis of the behaviour of crackemanating from microvoid in cement of reconstructed acetabulum Materials Science and Engineering: A, Vol-ume 457, Issues 1-2, 25 May Pages 385-391.

[14] Simin, Li. Adel Abdel-Wahab. Emrah Demirci, Vadim V. Silberschmidt. 2013. "Fracture process in cortical bone: X-FEM analysis of microstructured models" DOI 10.1007/978-3-319-04397-5_5.

[15] Kayabasi, O. and Erzincanli, F. 2006. Finite element modelling and analysis of a new cemented hip prosthesis. Advances in Engineering Software, 37(7), 477–483.

[16] Monif, M.M. 2012. Finite element study on the predicted equivalent stresses in the artificial hip joint. Journal of Biomed-ical Science and Engineering, 5, 43-51.

[17] Darwish, S.M. and Al-Samhan, A.M. 2009. Optimization of Artificial Hip Joint Parameters. Mat.-wiss. u. Werkstofftech, 40(3), 218-223.

[18] Bergmann, G. 2001. "HIP98", Free University, BerLin: ISBN 3-9807848-0-0.

[19] Ridha, Hambli. 2013. "finite element prediction of proximal femur fracture pattern based on orthotropic behaviour law coupled to quasi-damage,"medical engineering and physics 34. 202-210.

[20] Hugo, Giambini.; Xiaoliang, Qin.; Dan Dragomir‐Daescu.; Kai‐Nan An.; Ahmad Nassr.2015."Specimen‐specific vertebral fracture modeling: a feasibility study using the extended finite element method" Med Biol Eng Comput. DOI 10.1007/s11517-015-1348.

[21] Zhengdong Li. 2013. "Finite element analysis of pedestrian lower limb fractures by direct force: the result of being run over or impact," forensic science international 229 43-51.

[22] Adel, A. Abdel-Wahab. Angelo, R. Maligno, Vadim V. Silberschmidt. 2012. "Micro-scale modelling of bovine cortical bone fracture: Analysis

of crack propagation and microstructure using X-FEM" Computational Materials Science 52 128–135.

[23] Morgan, E.F.; Keaveny, T.M. 2001. Dependence of yield strain of human trabecular bone on anatomic site. Journal of Biomechanics 34, 569–77.

[24] Dassault Systèmes. 2013.Abaqus v6.13 Documentation-ABAQUS analysisuser'smanual. ABAQUS Inc; 6.13.

[25] Susan, Mischinski.; Ani, Ural. 2013. "Interaction of microstructure and microcrack growth in cortical bone: a finite ele-ment study" Computer Methods in Biomechanics and Biomedical Engineering, Vol. 16, No. 1, 81–94.

[26] Azhar A. Ali. 2014. "Specimen-specific modeling of hip fracture pattern and repair" Journal of Biomechanics 47.536–543.

[27] Jai Hyung Park, Yongkoo Lee, Oog-Jin Shon, Hyun Chul Shon, Ji Wan Kim. 2016. Surgical tips of intramedullary nailing in severely bowed femurs in atypical femur fractures: Simulation with 3D printed model. Injury, Int. J. Care Injured 47.1318–1324.